



Published in final edited form as:

Cell Rep. 2018 April 03; 23(1): 1–10. doi:10.1016/j.celrep.2018.03.025.

Loss of Dnmt3a Immortalizes Hematopoietic Stem Cells *In Vivo*

Mira Jeong^{1,9}, Hyun Jung Park^{2,9}, Hamza Celik^{3,9}, Elizabeth L. Ostrander³, Jaime M. Reyes⁴, Anna Guzman¹, Benjamin Rodriguez², Yong Lei¹, Yeojin Lee⁵, Lei Ding⁵, Olga A. Guryanova⁶, Wei Li^{2,7}, Margaret A. Goodell^{1,4,*}, and Grant A. Challen^{3,8,10,*}

¹Stem Cells and Regenerative Medicine Center, Baylor College of Medicine, Houston, TX 77030, USA

²Dan L. Duncan Cancer Center, Baylor College of Medicine, Houston, TX 77030, USA

³Division of Oncology, Department of Medicine, Washington University School of Medicine, St. Louis, MO 63110, USA

⁴Department of Molecular and Human Genetics, Baylor College of Medicine, Houston, TX 77030, USA

⁵Columbia Stem Cell Initiative, Department of Rehabilitation and Regenerative Medicine, Department of Microbiology and Immunology, Columbia University Medical Center, New York, NY 10032, USA

⁶Department of Pharmacology and Therapeutics, University of Florida College of Medicine, and UF Health Cancer Center, Gainesville, FL 32610, USA

⁷Department of Molecular and Cellular Biology, Baylor College of Medicine, Houston, TX 77030, USA

⁸Developmental, Regenerative and Stem Cell Biology Program, Division of Biology and Biomedical Sciences, Washington University School of Medicine, St. Louis, MO 63110, USA

This is an open access article under the CC BY-NC-ND license (<http://creativecommons.org/licenses/by-nc-nd/4.0/>).

*Correspondence: goodell@bcm.edu (M.A.G.), gchallen@dom.wustl.edu (G.A.C.).

⁹These authors contributed equally

¹⁰Lead Contact

DATA AND SOFTWARE AVAILABILITY

The accession number for the raw and processed whole-genome bisulfite sequencing (WGBS), histone modification, and RNA sequencing data reported in this paper is GEO: GSE98191. UCSC Genome Browser tracks (mouse mm9) can be accessed from the hub <http://lilab.research.bcm.edu/dldcc-web/lilab/hjpark/multipleTransplants/hub.txt>. The accession number for the exome sequencing data reported in this paper is SRA: SRP133364.

SUPPLEMENTAL INFORMATION

Supplemental Information includes Supplemental Experimental Procedures, four figures, and four tables and can be found with this article online at <https://doi.org/10.1016/j.celrep.2018.03.025>.

DECLARATION OF INTERESTS

The authors declare no competing interests.

AUTHOR CONTRIBUTIONS

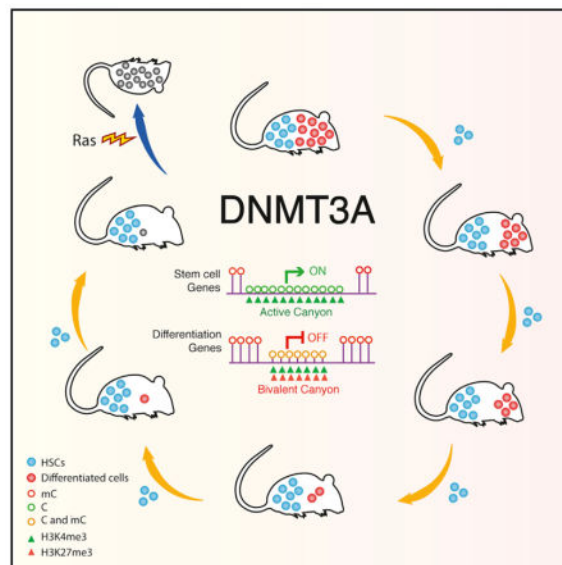
Conceptualization, G.A.C.; Methodology, M.J., H.J.P., H.C., Y. Lee, W.L., M.A.G., and G.A.C.; Software, H.J.P., J.M.R., B.R., and W.L.; Validation, M.J., H.J.P., M.A.G., and G.A.C.; Formal Analysis, M.J., H.J.P., J.M.R., B.R., M.A.G., and G.A.C.; Investigation, M.J., H.C., E.L.O., A.G., Y. Lei, and G.A.C.; Resources, L.D., O.A.G., W.L., M.A.G., and G.A.C.; Data Curation, H.J.P., W.L., M.A.G., and G.A.C.; Writing – Original Draft Preparation, M.J., H.J.P., H.C., and G.A.C.; Writing – Review & Editing, M.A.G. and G.A.C.; Visualization, M.J., H.J.P., H.C., E.L.O., M.A.G., and G.A.C.; Supervision, M.A.G. and G.A.C.; Project Administration, M.A.G. and G.A.C.; Funding Acquisition, M.A.G. and G.A.C.

SUMMARY

Somatic mutations in DNMT3A are recurrent events across a range of blood cancers. Dnmt3a loss of function in hematopoietic stem cells (HSCs) skews divisions toward self-renewal at the expense of differentiation. Moreover, DNMT3A mutations can be detected in the blood of aging individuals, indicating that mutant cells outcompete normal HSCs over time. It is important to understand how these mutations provide a competitive advantage to HSCs. Here we show that Dnmt3a-null HSCs can regenerate over at least 12 transplant generations in mice, far exceeding the lifespan of normal HSCs. Molecular characterization reveals that this *in vivo* immortalization is associated with gradual and focal losses of DNA methylation at key regulatory regions associated with self-renewal genes, producing a highly stereotypical HSC phenotype in which epigenetic features are further buttressed. These findings lend insight into the preponderance of DNMT3A mutations in clonal hematopoiesis and the persistence of mutant clones after chemotherapy.

In Brief

Jeong et al. show that a single genetic manipulation, conditional inactivation of the DNA methyltransferase enzyme Dnmt3a, removes all inherent hematopoietic stem cell (HSC) self-renewal limits and replicative lifespan. Deletion of Dnmt3a allows HSCs to be propagated indefinitely *in vivo*.



INTRODUCTION

Embryonic stem cells (ESCs) can be propagated indefinitely *in vitro* while maintaining their defining stem cell properties of self-renewal and differentiation. However, self-renewal of somatic stem cells such as hematopoietic stem cells (HSCs) appears to have a limit, as serial transplantation invariably results in loss of repopulation ability (Micklem et al., 1987; Siminovitch et al., 1964; Harrison and Astle, 1982). Understanding these limitations is

important for dissecting stem cell regulation and developing strategies to expand HSCs *ex vivo* for cell and gene therapy applications.

We previously showed that genetic inactivation of de novo DNA methyltransferase 3a (*Dnmt3a*) enhances self-renewal of murine HSCs (Challen et al., 2011, 2014). In humans, mutations in *DNMT3A* have been associated with clonal hematopoiesis of indeterminate potential (CHIP) in aging individuals (Genovese et al., 2014; Jaiswal et al., 2014; Xie et al., 2014). *DNMT3A* mutations in CHIP typically result in loss of activity through divergent mechanisms (Kim et al., 2013; Russler-Germain et al., 2014; Spencer et al., 2017), which probably confers enhanced self-renewal and enables them to slowly outcompete their normal counterparts over a long timescale.

Although loss of *Dnmt3a* promotes self-renewal, the degree of enhancement is undefined. Given that *DNMT3A* mutations are frequent in hematologic malignancies (Yang et al., 2015), are associated with a pre-malignant state (Shlush et al., 2014; Corces-Zimmerman et al., 2014), and can repopulate after chemotherapy (Pløen et al., 2014), it is critical to understand the mechanisms of resilience and longevity of *DNMT3A* mutant HSCs. Here we rigorously examine the replicative limits of HSCs lacking *Dnmt3a*.

RESULTS

Loss of *Dnmt3a* Provides HSCs with Indefinite Longevity

We previously showed that *Dnmt3a*-null (Mx1-Cre:*Dnmt3a*^{fl/fl} HSCs treated with pIpC = *Dnmt3a*^{KO}) HSCs could self-renew for up to four rounds of serial transplantation (Challen et al., 2011). We terminated these experiments after four transplants because control HSCs failed to self-renew past this point. However, as *Dnmt3a*^{KO} HSCs continued to show robust HSC repopulation, we hypothesized that *Dnmt3a* loss of function may remove inherent constraints on HSC self-renewal and longevity. Here, we tested these limits. Phenotypic HSCs (Lineage⁻ c-Kit⁺ Sca-1⁺ CD48⁻ CD150⁺ CD45.2⁺) were purified from prior recipients (CD45.1⁺) using flow cytometry. Two hundred HSCs were re-injected along with fresh whole bone marrow (WBM) competitor cells (CD45.1⁺) into new recipients (Figure 1A). Eighteen to 24 weeks later, recipients were sacrificed for analysis and continued HSC transplantation. After each transplant round, donor-derived (CD45.2⁺) HSCs were quantified (Figure 1B). After the third transplant, *Dnmt3a*^{KO} HSCs failed to generate substantial peripheral blood progeny (Figures 1C and 1D). Nevertheless, robust repopulation of *Dnmt3a*^{KO} HSCs was readily detectable in the bone marrow of recipient mice over 12 rounds of transplantation (Figure 1D). These HSCs displayed all the canonical markers of long-term HSCs (Figure S1A), and the expanded population was highly restricted to the HSC pool (Figure S1B). This degree of self-renewal far exceeds the potential of normal HSCs.

When *Dnmt3a*^{KO} HSCs are forced to differentiate in the absence of WBM competitor cells, a variety of hematopoietic pathologies arise (Celik et al., 2015; Mayle et al., 2015). To determine whether the immortalized HSCs were transformed, we transplanted 1×10^5 ninth-generation transplant (Tx-9) *Dnmt3a*^{KO} HSCs without competitor WBM. These animals succumbed to bone marrow failure (Figure 1E) with anemia and peripheral cytopenias

(Figure 1F), likely resulting from the inability of *Dnmt3a*^{KO} HSCs to generate sufficient blood elements to sustain the recipients in the absence of wild-type (WT) support cells. Bone marrow histology (data not shown) showed no evidence of leukemic transformation. Expanded *Dnmt3a*^{KO} HSCs were not mobilized in the blood (Figure S1C), and no extramedullary hematopoiesis was observed in the spleen (Figure S1D). Mice transplanted with control or *Dnmt3a*^{KO} HSCs contained similar numbers of stromal cells (Figure S1E) and appropriate bone marrow localization (Figure S1F). *Dnmt3a*^{KO} HSCs showed similar proximity to endothelial cells as control HSCs (Figure S1G) but were found to be closer to neighboring HSCs (Figure S1H), as would be expected from their clonal expansion.

***Dnmt3a* Controls DNA Methylation at HSC Regulatory Elements**

We performed molecular comparisons of age-matched control and early-stage transplant *Dnmt3a*^{KO} HSCs with late-stage transplant *Dnmt3a*^{KO} HSCs. Global DNA methylation analysis (Figure S2A; Table S1) showed that Tx-11 *Dnmt3a*^{KO} HSCs retained their overall methylation profile, with the majority of CpGs still methylated throughout the genome, but displayed DNA hypomethylation compared with control HSCs. This pattern was similar to, but more exaggerated than, the depletion of DNA methylation in early-stage transplant (Tx-3) *Dnmt3a*^{KO} HSCs (Figure 2A).

Differentially methylated regions (DMRs) were defined as more than three CpGs within 300 bp that show >20% methylation change in the same direction. Of the genomic regions showing differential methylation both in Tx-3 *Dnmt3a*^{KO} (to age-matched WT) and Tx-11 *Dnmt3a*^{KO} (versus Tx-3) HSCs, 556 regions hypermethylated in Tx-3 were equally as likely to gain (297) or lose (259) DNA methylation in Tx-11 *Dnmt3a*^{KO} HSCs (Figure 2B), suggesting that this hypermethylation was not stable. Conversely, 4,313 of 4,986 regions (86.5%) of the genome that lost DNA methylation in early-passage *Dnmt3a*^{KO} HSCs (hypo-DMRs) showed a trend toward continued loss of methylation in later stage transplant *Dnmt3a*^{KO} HSCs. There was significant enrichment for these “hypo_hypo” DMRs in stem cell enhancer elements (Figure 2C), but not CpG islands or gene promoters. “Hypo_hypo” DMRs were also enriched for transcription factor binding sites (TFBSs; Figure S2B), including hematopoietic regulators such as *Gata2* (Figure S2C). This enrichment was not due to the difference in DMR numbers, as 100 random computational samplings of 600 “hypo_hypo” and “hypo_hyper” DMRs showed the same trend (Figure S2D).

Because loss of DNA methylation in *Dnmt3a*^{KO} HSCs is particularly concentrated in DNA methylation canyons (Jeong et al., 2014), we examined canyons in late-passage HSCs. There are 1,093 canyons in WT HSCs (Jeong et al., 2014), which can be subdivided on the basis of histone marks into 565 active (H3K4me3⁺), 205 bivalent (H3K4me3⁺ H3K27me3⁺), and 323 inactive (H3K27me3⁺) canyons. Targeted loss of DNA methylation at active canyon walls was previously noted in early-passage *Dnmt3a*^{KO} HSCs (Jeong et al., 2014). In Tx-11 *Dnmt3a*^{KO} HSCs, there was further erosion of these walls (Figure 2D), and hypomethylation extended from the canyon edges (Figure S2E). In contrast, bivalent and inactive canyons displayed increased DNA methylation in Tx11 *Dnmt3a*^{KO} HSCs (Figure 2E) and no changes in the canyon border region (Figure S2E). Hypermethylation of inactive canyons did not lead to altered gene expression, as these genes are typically expressed at negligible levels (Figure

2F). However, genes in bivalent canyons, exemplified by *Cxcl12* (Figure 2E), showed repression following hypermethylation with extended passage. As many genes contained in such canyons are important for HSC lineage commitment, this hypermethylation may be a mechanism that inhibits differentiation of the mutant HSCs.

RNA sequencing (RNA-seq) was performed to determine the impact of DNA methylation changes on gene expression. In general, genes that were differentially expressed between control and Tx-3 *Dnmt3a*^{KO} HSCs showed similar expression patterns in Tx-9 *Dnmt3a*^{KO} HSCs (Figure S2F). We noted previously that early-passage *Dnmt3a*^{KO} HSCs exhibited increased expression of genes associated with HSC identity (Challen et al., 2011), defined as “HSC fingerprint” genes (Chambers et al., 2007). This trend continued in Tx-9 *Dnmt3a*^{KO} HSCs. Although the majority of HSC fingerprint genes are upregulated in mutant HSCs, exceptions include several imprinted genes (Figure S2G) such as *Ndn*, *Gtl2*, and *Peg3* implicated in stem cell function (Kubota et al., 2009; Qian et al., 2016; Berg et al., 2011). In summary, lack of *Dnmt3a* over serial passage stabilizes the self-renewing epigenome and leads to an inability to silence genes associated with maintenance of HSC identity.

Differentiation Capacity Is Lost but Transformation Potential Is Retained in Immortalized *Dnmt3a*^{KO} HSCs

We rescued late-passage *Dnmt3a*^{KO} HSCs with enforced expression of *Dnmt3a* to determine if differentiation capacity could be restored. Tx-11 *Dnmt3a*^{KO} HSCs were transduced with a lentivirus expressing full-length *Dnmt3a* (with bicistronic GFP) and transplanted. Re-expression of *Dnmt3a* led to the emergence of GFP⁺ cells in the peripheral blood at 4 weeks post-transplant (Figures S3A and S3B), which was not observed from transduction of the same HSCs with the control lentivirus. But ultimately, this initial output was not sustained (Figure S3C). However, ectopic expression of *Dnmt3a* did abrogate clonal expansion of the mutant HSCs in the bone marrow (Figure 3A). Although the total HSC frequency was identical in recipients of *Dnmt3a*^{KO} HSCs transduced with control or *Dnmt3a*-expressing lentivirus, GFP⁺ HSCs were severely depleted when expression of *Dnmt3a* was restored (Figure 3B). Re-expression of *Dnmt3a* induced proliferation (Figures 3C and S3D) and increased apoptosis (Figures 3D and S3E), which was associated with upregulation of the pro-apoptotic genes *Bbc3* (*puma*) and *Bax* (Figure 3E).

To evaluate differentiation capacity without cellular competition, myeloid potential of GFP⁺ *Dnmt3a*^{KO} HSCs was quantified by colony-forming assay. Myeloid potential of Tx-12 *Dnmt3a*^{KO} HSCs was severely compromised, and their differentiation was not rescued by complementation with *Dnmt3a*-expressing lentivirus (Figure 3F). Moreover, the colonies that were produced by late-passage *Dnmt3a*^{KO} HSCs were predominantly uni-lineage (Figure 3F). Similarly, re-expression of *Dnmt3a* was not able to restore T cell potential on OP9-DL1 co-culture (Schmitt and Zúñiga-Pflücker, 2002). Although *Dnmt3a* expression increased CD4⁺ T cell production, this output was marginal compared with control and early-passage *Dnmt3a*^{KO} HSCs (Figure S3F). But analysis of the double-negative (DN; CD4⁻ CD8a⁻) population did show development through the early stages of T cell maturation. In fact, re-expression of *Dnmt3a* generated an abnormal CD25^{bright} DN2 cell

population (Figure S3G), consistent with our observation that *Dnmt3a* is necessary for developmental progression of T cell progenitors (Kramer et al., 2017).

We then considered whether differentiation could bypass *Dnmt3a*. *Ebf1* is a master regulator of B cell potential (Lin and Grosschedl, 1995) located in a canyon that becomes hypermethylated with extended passage of *Dnmt3a*^{KO} HSCs. Tx-12 *Dnmt3a*^{KO} HSCs were transduced with control, *Dnmt3a*-expressing, or *Ebf1*-expressing lentivirus and co-cultured on OP9 stromal cells for 14 days. The B cell (B220⁺ CD19⁺) differentiation deficit in early-passage *Dnmt3a*^{KO} HSCs was restored by expression of *Dnmt3a*, and like control HSCs, B cell output of early-passage *Dnmt3a*^{KO} HSCs was enhanced by overexpression of *Ebf1* (Figure 3G). In contrast, overexpression of neither *Dnmt3a* nor *Ebf1* was able to restore any B cell potential to late-passage *Dnmt3a*^{KO} HSCs (Figure 3G).

If differentiation potential was completely silenced, perhaps immortalized *Dnmt3a*^{KO} HSCs would be incapable of malignant transformation, given that some differentiation is required for generation of acute myeloid leukemia (AML) (Ye et al., 2015). Tx-12 *Dnmt3a*^{KO} HSCs were transduced with a lentivirus expressing *Kras*^{G12D}, a common mutation co-occurring with *DNMT3A* mutations in AML (Ley et al., 2013), and transplanted. Once GFP⁺ cells began emerging in the blood, mice rapidly succumbed (Figure 3H) to a fully penetrant AML with a c-Kit⁺ CD11b⁺ phenotype (Figure 3I). Thus, although differentiation was irreversibly blocked in immortalized *Dnmt3a*^{KO} HSCs, they retained the potential for malignant transformation when presented with an appropriate co-operating mutation.

Molecular Analysis of *Dnmt3a* Rescue, Dominant-Negative Mutant, and Clonal Hematopoiesis

DNA methylation was compared between Tx-12 *Dnmt3a*^{KO} HSCs transduced with either control or *Dnmt3a*-expressing lentivirus. Of 361 genomic regions hypomethylated in Tx-11 *Dnmt3a*^{KO} HSCs versus Tx-3 *Dnmt3a*^{KO} HSCs, 280 (77.6%) became hypermethylated in Tx-12 *Dnmt3a*^{KO} HSCs following re-expression of *Dnmt3a*, indicating that DNA methylation was re-established at the correct regions, including canyon boundaries (Figure 4A) and enhancers (Figure 4B). The re-establishment of DNA methylation patterns did not necessarily correlate with corresponding gene expression differences (Figure S4A), but perhaps this would be normalized with further re-expression of *Dnmt3a* (Figure S4B).

We also compared the DNA methylation changes in *Dnmt3a*^{KO} HSCs with those in the context of mutations in patients. The most prevalent *DNMT3A* mutation is a missense at amino acid 882 (Ley et al., 2010). This mutation creates a dominant-negative protein with reduced DNA methyltransferase capacity (Russler-Germain et al., 2014; Kim et al., 2013). Global DNA methylation was performed on Tx-3 *Dnmt3a*^{R878H/+} HSCs (*Dnmt3a*^{R878}; mouse homolog of human *DNMT3A*^{R882H}) (Guryanova et al., 2016) and compared with Tx-3 *Dnmt3a*^{KO} HSCs. Tx-3 *Dnmt3a*^{R878} HSCs displayed a self-renewal advantage over control HSCs, but not to the same degree as *Dnmt3a*^{KO} HSCs (Figure S4C). On a global scale, *Dnmt3a*^{R878} showed hypomethylation throughout the genome, although not to the same degree as *Dnmt3a*^{KO} HSCs (Figure 4C). There was high correlation between the regions affected by changes in DNA methylation in *Dnmt3a*^{R878} and *Dnmt3a*^{KO} HSCs. Of the DMRs shared between *Dnmt3a*^{R878} and *Dnmt3a*^{KO} HSCs compared with WT, 95.0%

(1,653 of 1,730) showed hypermethylation in both mutant genotypes, while 95.6% (6,742 of 7,032) underwent hypomethylation in both mutant HSC genotypes. Of the 12,644 hypo-DMRs in *Dnmt3a*^{R878} HSCs compared with WT, 6,724 (53.2%) are hypo-DMRs in *Dnmt3a*^{KO} HSCs at the exact same genomic co-ordinates, with this fraction increasing if the genome windows are extended. Although overall methylation patterns were highly overlapping between the *Dnmt3a* mutant HSCs, there were distinct focal changes. For example, *Dnmt3a*^{R878} HSCs did not exhibit the hypermethylation of enhancer elements of differentiation factors such as *Pax5* and *Bcl11b* (Figure S4D). Similarly, the *HoxB* gene cluster, which becomes significantly hypomethylated in *Dnmt3a*^{KO} HSCs, did not show the same loss of DNA methylation in *Dnmt3a*^{R878} HSCs (Figure 4E) and corresponding transcriptional upregulation (Figure 4F). A CpG island in the *Gata3* promoter is particularly sensitive to *Dnmt3a* loss of function (Challen et al., 2011), but DNA methylation remained intact for this region in *Dnmt3a*^{R878} HSCs (Figure 4G), and gene expression was unchanged (Figure 4H). These findings suggest that *Dnmt3a*^{KO} and *Dnmt3a*^{R878H} mutations in HSCs result in similar overall DNA methylation changes, but methylation differences at specific stem cell enhancer elements may be important for the differentiation defects in the loss-of-function model.

The expansion of *Dnmt3a*^{KO} HSCs over extended passage was reminiscent of human CHIP, which can persist in a benign state for decades. To determine if this HSC expansion was associated with acquisition of co-operating mutations, exome sequencing was performed. The overall number of somatic variants was reduced in Tx-12 *Dnmt3a*^{KO} HSCs compared with early-passage HSCs (Figure 4I), but the variant allele fraction (VAF) of these variants was higher (Figure 4J), indicating the transplanted HSC pool was becoming more homogeneous over time. A reduced number of variants is consistent with reduced clonal complexity, while an increase in the VAF of individual variants (Tx-3 *Dnmt3a*^{KO} HSCs = 0.2400, Tx-12 *Dnmt3a*^{KO} HSCs = 0.4381) is consistent with heterozygous polymorphisms originating from dominant clones. However, analysis of the high-confidence somatic variants did not identify any acquired mutations which have been associated with human CHIP (Table S4).

As *Dnmt3a* has been suggested to regulate telomeres (Gonzalo et al., 2006) and telomere shortening limits HSC transplantability (Allsopp et al., 2003), we computationally predicted telomere length (Ding et al., 2014). Tx-12 *Dnmt3a*^{KO} HSCs showed no erosion of telomere length (Figure S4E; Table S4). Cumulatively, these data suggest *Dnmt3a* loss of function is sufficient to bias HSC fate decisions and initiate the pre-malignant condition of CHIP but is not sufficient to drive malignant transformation.

DISCUSSION

Here we show that loss of *Dnmt3a* endows HSCs with immortality *in vivo*. The self-renewal potential of *Dnmt3a*^{KO} HSCs far exceeds that of normal HSCs and the lifespan of the mice from which they were derived. Our data establish that HSCs do not have an inherently finite lifespan but that loss of *Dnmt3a* augments epigenetic features that enforce self-renewal and enable HSCs to be propagated indefinitely. Further examination of the mechanisms perpetuating immortality in *Dnmt3a*^{KO} HSCs may provide a window for artificially

extending the lifespan of HSCs, an important biomedical application in the context of the aging human population.

The differentiation block of immortal *Dnmt3a*^{KO} HSCs cannot be rescued by re-expression of *Dnmt3a* or transcription factors such as *Ebf1*. But re-expression of *Dnmt3a* abrogated the self-renewal phenotype, suggesting the roles of Dnmt3a in self-renewal and differentiation can be uncoupled. Our data also demonstrate that malignant transformation is agnostic to DNA methylation state: both early-passage (Mayle et al., 2015; Celik et al., 2015) and late-passage (this study) *Dnmt3a*^{KO} HSCs will generate malignancies when an appropriate co-operating mutation is acquired. How oncogenic signals can overcome the differentiation block of *Dnmt3a*^{KO} HSCs to generate disease warrants further investigation.

Although we use an artificial system of serial transplantation, we consider the extent to which these insights may be extrapolated to humans. *DNMT3A* mutations are the most common mutation in CHIP (Xie et al., 2014; Jaiswal et al., 2014; Genovese et al., 2014), with increasing frequency with age (McKerrell et al., 2015; Young et al., 2016). But as CHIP is identified by assaying peripheral blood, if *DNMT3A* mutant human HSCs also show compromised differentiation, we predict the proportion of mutant HSCs in the bone marrow is underestimated by current studies. Our experiments are also distinct from the human scenario in that each transplant of *Dnmt3a*^{KO} HSCs contains fresh WT bone marrow replete with normal HSCs. In the aging human, WT HSCs diminish in function (Pang et al., 2011), offering less competition to emerging *DNMT3A* mutant clones. Even partial loss of *DNMT3A* function through weak heterozygous mutations, likely enables mutant HSCs to outcompete WT counterparts. We also show that a dominant-negative *Dnmt3a* mutation (R878) equivalent to the frequent human R882 mutation results in very similar DNA methylation changes to the null allele, suggesting most *DNMT3A* mutations likely produce similar molecular and cellular consequences at least at the level of clonal expansion.

The phenotype of *Dnmt3a*^{KO} HSCs is unique. Mutation of some other genes can enhance HSCs capacity (Rossi et al., 2012), but none can remove the inherent limits on self-renewal and replicative lifespan like *Dnmt3a*. Our data add to the emerging view that HSCs are in constant competition with their siblings. Perturbations that confer an advantage to one HSC over another will be selected depending on the specific context. With the enormous self-renewal capacity of *Dnmt3a*-null HSCs demonstrated here, a single mutant HSC in human bone marrow can outcompete WT counterparts over a period of many years, even if initially vastly outnumbered.

EXPERIMENTAL PROCEDURES

Further details and an outline of resources used in this work can be found in Supplemental Experimental Procedures.

Mice and Transplantation

All animal procedures were approved by Institutional Animal Care and Use Committees and performed in strict adherence to Washington University institutional guidelines. All mice were C57BL/6 background. Recipient CD45.1 mice (8–10 weeks of age; strain #002014;

The Jackson Laboratory) were given a split dose of 10.5 Gy irradiation. Mx1-Cre(+):*Dnmt3a*^{fl/fl} mice have been previously described by our group (Challen et al., 2011). Control mice were Mx1-Cre(+):*Dnmt3a*^{+/+} mice. Deletion of floxed alleles was induced by intraperitoneal injection of 300 µg pIpC (#p1530; Sigma-Aldrich) six times every other day in adult mice (10–12 weeks old). Equal numbers of male and female mice were used.

For competitive transplants, 200 HSCs (Lineage⁻[Gr-1, Mac-1, B220, CD3e, Ter119], c-Kit⁺, Sca-1⁺, CD48⁻, CD150⁺) were transplanted with 2.5×10^5 WT CD45.1 competitor bone marrow. For serial transplantation, 200 donor-derived HSCs were isolated from the previous recipients 18–24 weeks post-transplant and transplanted into new lethally irradiated recipients along with fresh WT competitor bone marrow. Recipients were bled through the retro-orbital route and analyzed for donor-derived lineage contribution by flow cytometry.

Quantification and Statistical Analysis

Statistical comparisons between groups were evaluated using Student's t test or ANOVA as appropriate using Prism 6 (GraphPad). All data are presented as mean \pm SE. Time to morbidity is presented in Kaplan-Meier survival curves and analyzed using the log-rank test. Statistical significance is denoted as **p* < 0.05, ***p* < 0.01, and ****p* < 0.001; *n* indicates the number of biological replicates within each group.

Supplementary Material

Refer to Web version on PubMed Central for supplementary material.

Acknowledgments

We thank the Siteman Cancer Center (Washington University, Core Grant CA91842) and the Dan L. Duncan Cancer Center (Baylor College of Medicine, Core Grant CA125123). This work was supported by NIH grants DK102428 (to G.A.C.), HG007538 and CA193466 (to W.L.), HL132074 (to L.D.), CA178191 (to O.A.G.), and DK092883, CA183252 and AG036695, and CPRIT RP140053 (to M.A.G.). M.J. was supported by grant 5T32DK60445. H.C. was supported by an American Society of Hematology scholar award. E.L.O. was supported by NIH grant 5T32CA113275. Y.L. is supported by a NYSTEM training grant. J.M.R. was supported by grant GM056929.

References

- Allsopp RC, Morin GB, DePinho R, Harley CB, Weissman IL. Telomerase is required to slow telomere shortening and extend replicative lifespan of HSCs during serial transplantation. *Blood*. 2003; 102:517–520. [PubMed: 12663456]
- Berg JS, Lin KK, Sonnet C, Boles NC, Weksberg DC, Nguyen H, Holt LJ, Rickwood D, Daly RJ, Goodell MA. Imprinted genes that regulate early mammalian growth are coexpressed in somatic stem cells. *PLoS ONE*. 2011; 6:e26410. [PubMed: 22039481]
- Celik H, Mallaney C, Kothari A, Ostrand EL, Eultgen E, Martens A, Miller CA, Hundal J, Klco JM, Challen GA. Enforced differentiation of *Dnmt3a*-null bone marrow leads to failure with *c-Kit* mutations driving leukemic transformation. *Blood*. 2015; 125:619–628. [PubMed: 25416276]
- Challen GA, Sun D, Jeong M, Luo M, Jelinek J, Berg JS, Bock C, Vasanthakumar A, Gu H, Xi Y, et al. *Dnmt3a* is essential for hematopoietic stem cell differentiation. *Nat Genet*. 2011; 44:23–31. [PubMed: 22138693]
- Challen GA, Sun D, Mayle A, Jeong M, Luo M, Rodriguez B, Mallaney C, Celik H, Yang L, Xia Z, et al. *Dnmt3a* and *Dnmt3b* have overlapping and distinct functions in hematopoietic stem cells. *Cell Stem Cell*. 2014; 15:350–364. [PubMed: 25130491]

- Chambers SM, Boles NC, Lin KY, Tierney MP, Bowman TV, Bradfute SB, Chen AJ, Merchant AA, Sirin O, Weksberg DC, et al. Hematopoietic fingerprints: an expression database of stem cells and their progeny. *Cell Stem Cell*. 2007; 1:578–591. [PubMed: 18371395]
- Corces-Zimmerman MR, Hong WJ, Weissman IL, Medeiros BC, Majeti R. Preleukemic mutations in human acute myeloid leukemia affect epigenetic regulators and persist in remission. *Proc Natl Acad Sci U S A*. 2014; 111:2548–2553. [PubMed: 24550281]
- Ding Z, Mangino M, Aviv A, Spector T, Durbin R. Consortium UK; UK10K Consortium. Estimating telomere length from whole genome sequence data. *Nucleic Acids Res*. 2014; 42:e75. [PubMed: 24609383]
- Genovese G, Kähler AK, Handsaker RE, Lindberg J, Rose SA, Bakhoum SF, Chambert K, Mick E, Neale BM, Fromer M, et al. Clonal hematopoiesis and blood-cancer risk inferred from blood DNA sequence. *N Engl J Med*. 2014; 371:2477–2487. [PubMed: 25426838]
- Gonzalo S, Jaco I, Fraga MF, Chen T, Li E, Esteller M, Blasco MA. DNA methyltransferases control telomere length and telomere recombination in mammalian cells. *Nat Cell Biol*. 2006; 8:416–424. [PubMed: 16565708]
- Guryanova OA, Shank K, Spitzer B, Luciani L, Koche RP, Garrett-Bakelman FE, Ganzel C, Durham BH, Mohanty A, Hoermann G, et al. DNMT3A mutations promote anthracycline resistance in acute myeloid leukemia via impaired nucleosome remodeling. *Nat Med*. 2016; 22:1488–1495. [PubMed: 27841873]
- Harrison DE, Astle CM. Loss of stem cell repopulating ability upon transplantation. Effects of donor age, cell number, and transplantation procedure. *J Exp Med*. 1982; 156:1767–1779. [PubMed: 6129277]
- Jaiswal S, Fontanillas P, Flannick J, Manning A, Grauman PV, Mar BG, Lindsley RC, Mermel CH, Burt N, Chavez A, et al. Age-related clonal hematopoiesis associated with adverse outcomes. *N Engl J Med*. 2014; 371:2488–2498. [PubMed: 25426837]
- Jeong M, Sun D, Luo M, Huang Y, Challen GA, Rodriguez B, Zhang X, Chavez L, Wang H, Hannah R, et al. Large conserved domains of low DNA methylation maintained by Dnmt3a. *Nat Genet*. 2014; 46:17–23. [PubMed: 24270360]
- Kim SJ, Zhao H, Hardikar S, Singh AK, Goodell MA, Chen T. A DNMT3A mutation common in AML exhibits dominant-negative effects in murine ES cells. *Blood*. 2013; 122:4086–4089. [PubMed: 24167195]
- Kramer AC, Kothari A, Wilson WC, Celik H, Nikitas J, Mallaney C, Ostrander EL, Eultgen E, Martens A, Valentine MC, et al. Dnmt3a regulates T-cell development and suppresses T-ALL transformation. *Leukemia*. 2017; 31:2479–2490. [PubMed: 28321121]
- Kubota Y, Osawa M, Jakt LM, Yoshikawa K, Nishikawa S. Necdin restricts proliferation of hematopoietic stem cells during hematopoietic regeneration. *Blood*. 2009; 114:4383–4392. [PubMed: 19770359]
- Ley TJ, Ding L, Walter MJ, McLellan MD, Lamprecht T, Larson DE, Kandoth C, Payton JE, Baty J, Welch J, et al. DNMT3A mutations in acute myeloid leukemia. *N Engl J Med*. 2010; 363:2424–2433. [PubMed: 21067377]
- Ley TJ, Miller C, Ding L, Raphael BJ, Mungall AJ, Robertson A, Hoadley K, Triche TJ Jr, Laird PW, Baty JD, et al. Cancer Genome Atlas Research Network. Genomic and epigenomic landscapes of adult de novo acute myeloid leukemia. *N Engl J Med*. 2013; 368:2059–2074. [PubMed: 23634996]
- Lin H, Grosschedl R. Failure of B-cell differentiation in mice lacking the transcription factor EBF. *Nature*. 1995; 376:263–267. [PubMed: 7542362]
- Mayle A, Yang L, Rodriguez B, Zhou T, Chang E, Curry CV, Challen GA, Li W, Wheeler D, Rebel VI, Goodell MA. Dnmt3a loss predisposes murine hematopoietic stem cells to malignant transformation. *Blood*. 2015; 125:629–638. [PubMed: 25416277]
- McKerrell T, Park N, Moreno T, Grove CS, Ponstingl H, Stephens J, Crawley C, Craig J, Scott MA, Hodgkinson C, et al. Understanding Society Scientific Group. Leukemia-associated somatic mutations drive distinct patterns of age-related clonal hemopoiesis. *Cell Rep*. 2015; 10:1239–1245. [PubMed: 25732814]

- Micklem HS, Lennon JE, Ansell JD, Gray RA. Numbers and dispersion of repopulating hematopoietic cell clones in radiation chimeras as functions of injected cell dose. *Exp Hematol.* 1987; 15:251–257. [PubMed: 3469105]
- Pang WW, Price EA, Sahoo D, Beerman I, Maloney WJ, Rossi DJ, Schrier SL, Weissman IL. Human bone marrow hematopoietic stem cells are increased in frequency and myeloid-biased with age. *Proc Natl Acad Sci U S A.* 2011; 108:20012–20017. [PubMed: 22123971]
- Pløen GG, Nederby L, Guldberg P, Hansen M, Ebbesen LH, Jensen UB, Hokland P, Aggerholm A. Persistence of DNMT3A mutations at long-term remission in adult patients with AML. *Br J Haematol.* 2014; 167:478–486. [PubMed: 25371149]
- Qian P, He XC, Paulson A, Li Z, Tao F, Perry JM, Guo F, Zhao M, Zhi L, Venkatraman A, et al. The Dlk1-Gtl2 locus preserves LT-HSC function by inhibiting the PI3K-mTOR pathway to restrict mitochondrial metabolism. *Cell Stem Cell.* 2016; 18:214–228. [PubMed: 26627594]
- Rossi L, Lin KK, Boles NC, Yang L, King KY, Jeong M, Mayle A, Goodell MA. Less is more: unveiling the functional core of hematopoietic stem cells through knockout mice. *Cell Stem Cell.* 2012; 11:302–317. [PubMed: 22958929]
- Russler-Germain DA, Spencer DH, Young MA, Lamprecht TL, Miller CA, Fulton R, Meyer MR, Erdmann-Gilmore P, Townsend RR, Wilson RK, Ley TJ. The R882H DNMT3A mutation associated with AML dominantly inhibits wild-type DNMT3A by blocking its ability to form active tetramers. *Cancer Cell.* 2014; 25:442–454. [PubMed: 24656771]
- Schmitt TM, Zúñiga-Pflücker JC. Induction of T cell development from hematopoietic progenitor cells by delta-like-1 in vitro. *Immunity.* 2002; 17:749–756. [PubMed: 12479821]
- Shlush LI, Zandi S, Mitchell A, Chen WC, Brandwein JM, Gupta V, Kennedy JA, Schimmer AD, Schuh AC, Yee KW, et al. HALT Pan-Leukemia Gene Panel Consortium. Identification of pre-leukaemic haematopoietic stem cells in acute leukaemia. *Nature.* 2014; 506:328–333. [PubMed: 24522528]
- Siminovitch L, Till JE, McCulloch EA. Decline in colony forming ability of marrow cells subjected to serial transplantation into irradiated mice. *J Cell Comp Physiol.* 1964; 64:23–31. [PubMed: 14200349]
- Spencer DH, Russler-Germain DA, Ketkar S, Helton NM, Lamprecht TL, Fulton RS, Fronick CC, O’Laughlin M, Heath SE, Shinawi M, et al. CpG island hypermethylation mediated by DNMT3A is a consequence of AML progression. *Cell.* 2017; 168:801–816. e13. [PubMed: 28215704]
- Xie M, Lu C, Wang J, McLellan MD, Johnson KJ, Wendl MC, McMichael JF, Schmidt HK, Yellapantula V, Miller CA, et al. Age-related mutations associated with clonal hematopoietic expansion and malignancies. *Nat Med.* 2014; 20:1472–1478. [PubMed: 25326804]
- Yang L, Rau R, Goodell MA. DNMT3A in haematological malignancies. *Nat Rev Cancer.* 2015; 15:152–165. [PubMed: 25693834]
- Ye M, Zhang H, Yang H, Koche R, Staber PB, Cusan M, Levantini E, Welner RS, Bach CS, Zhang J, et al. Hematopoietic differentiation is required for initiation of acute myeloid leukemia. *Cell Stem Cell.* 2015; 17:611–623. [PubMed: 26412561]
- Young AL, Challen GA, Birman BM, Druley TE. Clonal haematopoiesis harbouring AML-associated mutations is ubiquitous in healthy adults. *Nat Commun.* 2016; 7:12484. [PubMed: 27546487]

Highlights

- Serial propagation of HSCs for 12 transplant generations, over 60 months in vivo
- Augmentation of modifications at enhancers and canyons to buttress self-renewal
- Differentiation becomes irreversibly compromised, but transformation potential remains

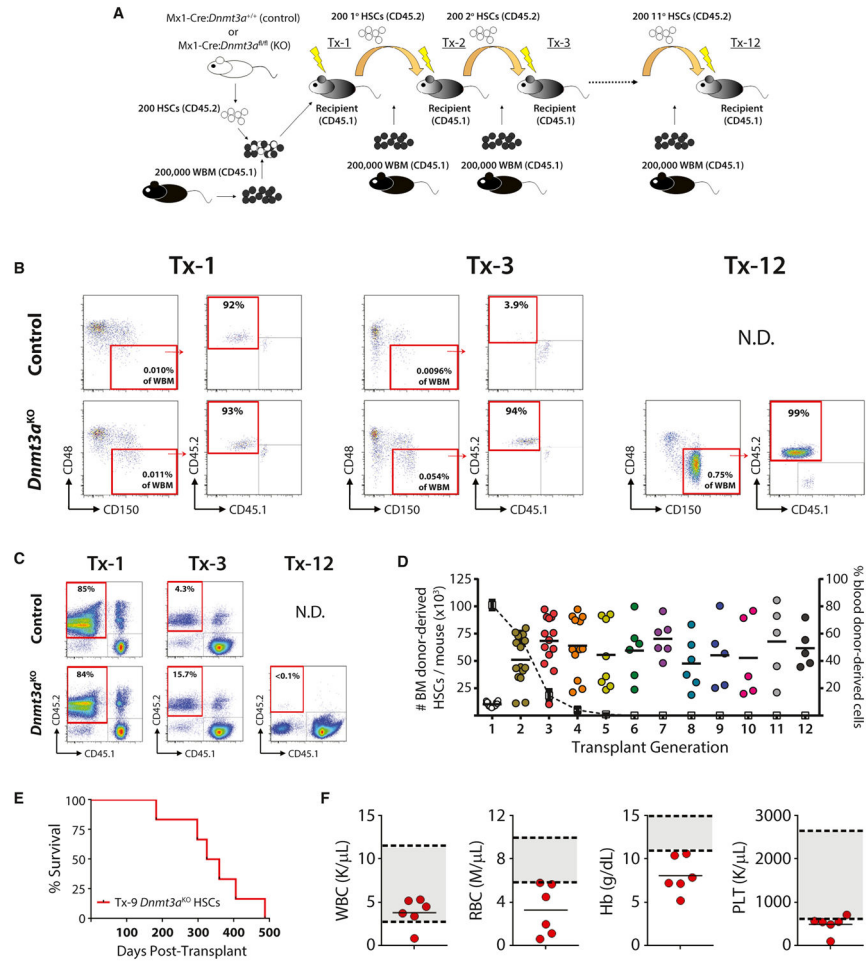


Figure 1. Loss of Dnmt3a Provides HSCs with Indefinite Longevity

(A) Schematic representation of serial HSC transplantation process. Tx, transplant stage; HSCs, hematopoietic stem cells; WBM, whole bone marrow.

(B and C) Representative flow cytometry plots showing donor-derived cell (CD45.2⁺) contribution to bone marrow HSC compartment (B) and peripheral blood (C) at the end of indicated stage of transplantation. N.D., not determined.

(D) Quantification of donor HSC-derived peripheral blood chimerism (dashed gray line) compared with absolute number of donor-derived HSCs per mouse generated from Dnmt3a^{KO} HSCs at the end of each transplant (n = 5–29 recipients per transplant generation).

(E) Time to morbidity in mice transplanted with 1 × 10⁵ Dnmt3a^{KO} HSCs in the absence of WBM competitor cells.

(F) Blood counts from moribund mice showing leukopenia, anemia, and thrombocytopenia. Gray shaded areas indicate normal range for WT mice.

See also Figure S1.

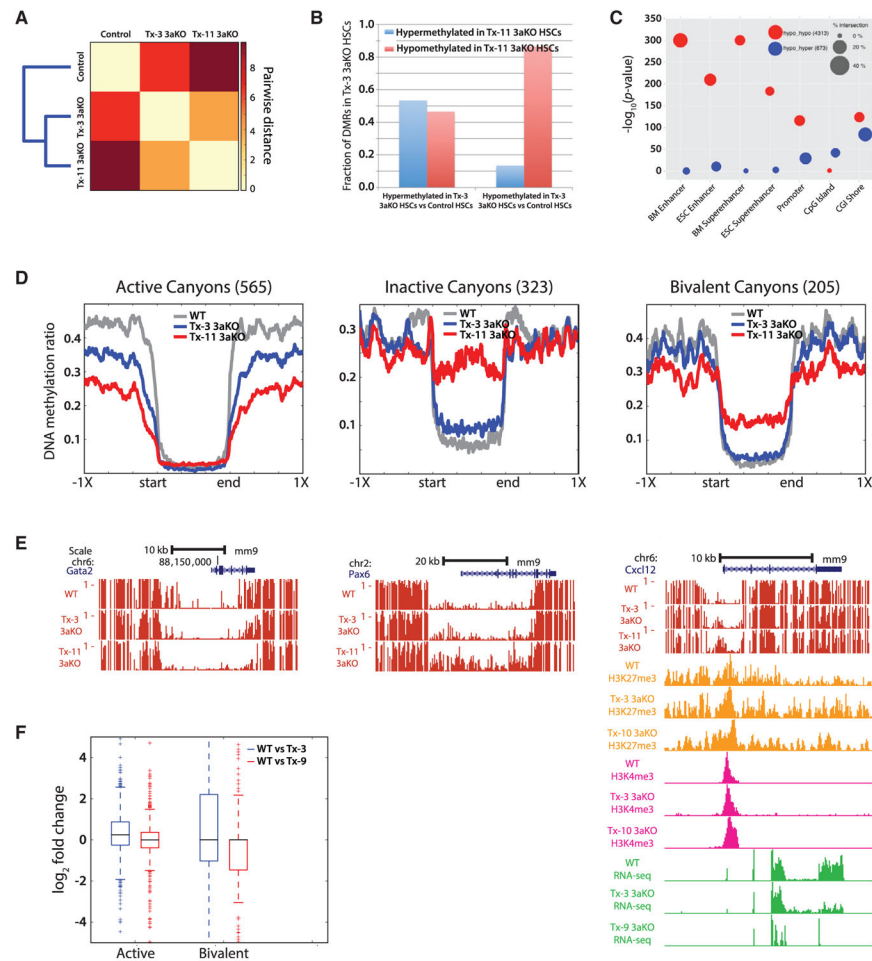


Figure 2. Dnmt3a Controls DNA Methylation at HSC Regulatory Elements

(A) Hierarchical clustering on the basis of CpG methylation ratio of control, Tx-3, and Tx-11 *Dnmt3a*^{KO} HSCs.

(B) Fraction of hyper- or hypo-methylated DMRs in Tx-3 *Dnmt3a*^{KO} HSCs (versus control HSCs) that became further hyper- or hypo-methylated in Tx-11 *Dnmt3a*^{KO} HSCs (versus Tx-3 *Dnmt3a*^{KO} HSCs).

(C) Enrichment analysis of 4,313 “hypo_hypo” regions compared with 673 control regions (“hypo_hyper”). Size of data points represents the overlap percentage with the size of the corresponding regulatory regions in the denominator.

(D) DNA methylation levels of active, bivalent, and inactive canyons in control (WT), Tx-3 *Dnmt3a*^{KO}, and Tx-11 *Dnmt3a*^{KO} HSCs. Flanking regions are extended by the same length as the corresponding canyon ($\pm 1\times$).

(E) DNA methylation profile of active, inactive, and bivalent canyon loci by WGBS. The height of each bar represents the DNA methylation level of an individual CpG. Also shown for *Cxcl12* are histone marks defining bivalent canyons and RNA-seq expression.

(F) Expression level changes of genes within active and bivalent canyon regions. See also Figure S2.

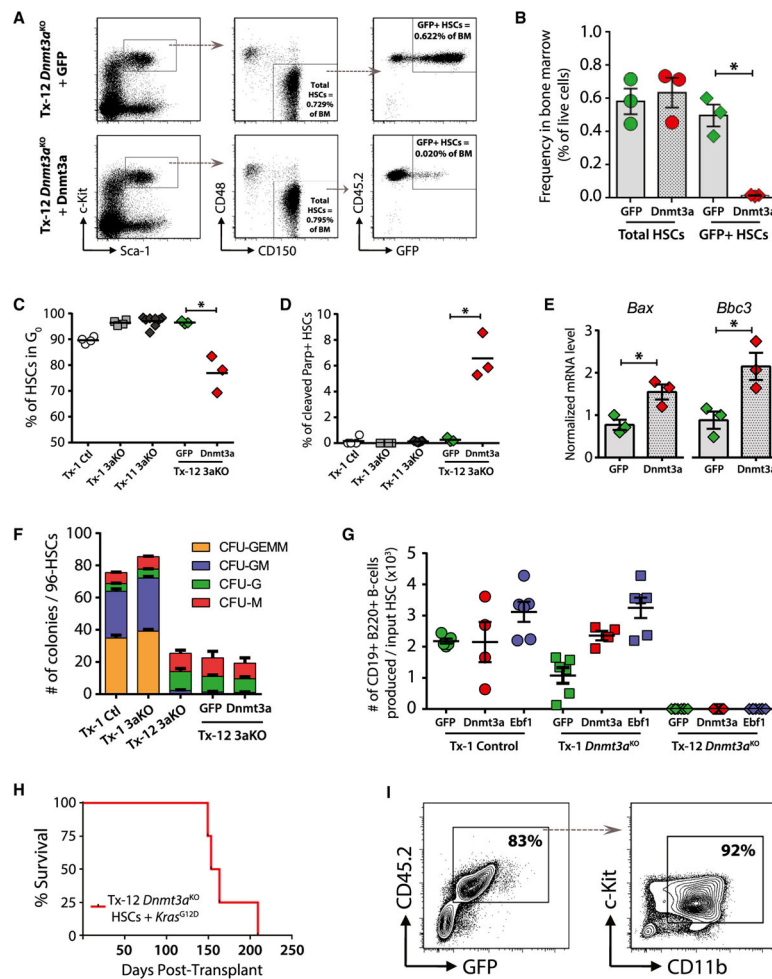


Figure 3. Differentiation Capacity Is Lost but Transformation Potential Is Retained in Immortalized *Dnmt3a*^{KO} HSCs

(A) Representative flow cytometry plots showing bone marrow analysis of mice transplanted with Tx-11 *Dnmt3a*^{KO} HSCs transduced with control (GFP) or *Dnmt3a*-expressing (*Dnmt3a*) lentivirus 18 weeks post-transplant.

(B) Frequency of transduced Tx-11 *Dnmt3a*^{KO} HSCs in bone marrow of recipient mice 18 weeks post-transplant.

(C) Cell cycle analysis of the indicated genotype/transplant stage showing proportion of quiescent (G₀) HSCs.

(D) Quantification of apoptotic HSCs of the indicated genotype/transplant stage.

(E) Expression of pro-apoptotic genes in Tx-11 *Dnmt3a*^{KO} HSCs transduced with control (GFP) or *Dnmt3a*-expressing (*Dnmt3a*) lentivirus.

(F) Clonogenic myeloid potential of HSCs from the indicated genotype/transplant stage.

(G) B cell potential of HSCs from the indicated genotype/transplant stage transduced with control (GFP), *Dnmt3a*-expressing, or *Ebf1*-expressing lentivirus.

(H) Time to morbidity in mice transplanted with Tx-12 *Dnmt3a*^{KO} HSCs transduced with lentivirus expressing *Kras*^{G12D}.

(I) Phenotype of *Kras*^{G12D}-driven AML.

Mean \pm SEM values are shown. * $p < 0.05$, ** $p < 0.01$. See also Figure S3.

Author Manuscript

Author Manuscript

Author Manuscript

Author Manuscript

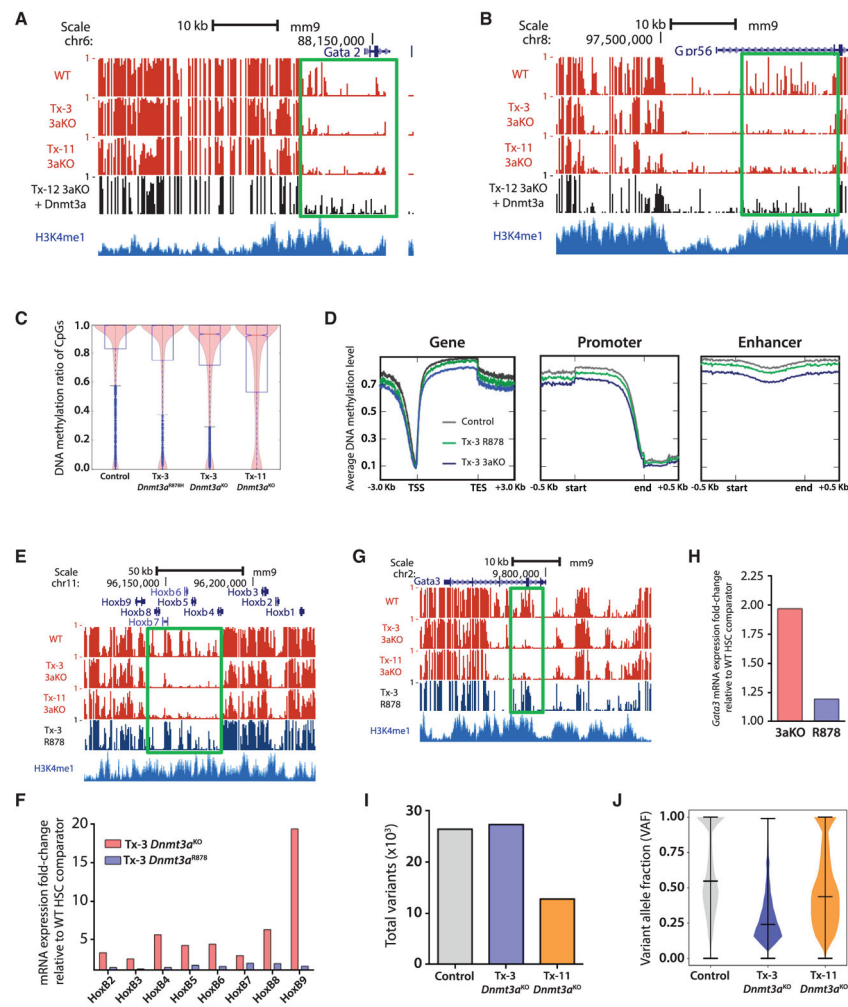


Figure 4. Molecular Analysis of *Dnmt3a* Rescue, Dominant-Negative Mutant, and Clonal Hematopoiesis

(A and B) WGBS profiles showing increased DNA methylation (green boxes) in *Gata2* canyon (A) and *Gpr56* enhancer (B) in Tx-11 *Dnmt3a*^{KO} HSCs transduced with *Dnmt3a*-expressing lentivirus.

(C) DNA methylation ratio of CpGs throughout the genome in HSCs of the indicated genotypes.

(D) Methylation levels of CpGs within gene bodies, promoters, and enhancers.

(E) DNA methylation profiles of the *HoxB* locus. Green box shows hypomethylation in *Dnmt3a*^{KO}, which is not observed in *Dnmt3a*^{R878} HSCs.

(F) Expression levels of *HoxB* genes in Tx-3 *Dnmt3a*^{KO} and Tx-3 *Dnmt3a*^{R878} HSCs. Data are expressed as relative fold change to control comparators in each sequencing experiment (n = 2–4 biological replicates per genotype).

(G and H) DNA methylation profile of *Gata3* locus showing hypomethylation of *Dnmt3a*^{KO} (3aKO) HSCs (green box) (G), corresponding with increased gene expression (H), not conserved in *Dnmt3a*^{R878} (R878) HSCs. Expression data are expressed as relative fold change to control comparators in each sequencing experiment (n = 2–4 biological replicates per genotype).

(I and J) Total number of somatic variants (I) and variant allele fraction (J) in HSCs from the indicated genotype/transplant stage.
See also Figure S4.

Author Manuscript

Author Manuscript

Author Manuscript

Author Manuscript